Effective Simulation Approach for Lightning Impulse Voltage Tests of Reactor and Transformer Windings

Piyapon Tuethong, Peerawut Yutthagowith * and Anantawat Kunakorn

Faculty of Engineering, King Mongkut's Institute of Technology Ladkrabang, Bangkok 10520, Thailand; t_piyapon@hotmail.com (P.T.); anantawat.ku@kmitl.ac.th (A.K.)

* Correspondence: kypeeraw@kmitl.ac.th; Tel.: +66-(0)2-329-8330

check for updates

Abstract: In this paper, an effective simulation method for lightning impulse voltage tests of reactor and transformer windings is presented. The method is started from the determination of the realized equivalent circuit of the considered winding in the wide frequency range from 10 Hz to 10 MHz. From the determined equivalent circuit and with the use of the circuit simulator, the circuit parameters in the impulse generator circuit are adjusted to obtain the waveform parameters according to the standard requirement. The realized equivalent circuits of windings for impulse voltage tests have been identified. The identification approach starts from equivalent circuit determination based on a vector fitting algorithm. However, the vector fitting algorithm with the equivalent circuit extraction is not guaranteed to obtain the realized equivalent circuit. From the equivalent circuit, it is possible that there are some negative parameters of resistance, inductance, and capacitance. Using such circuit parameters from the vector fitting approach as the beginning circuit parameters, a genetic algorithm is employed for searching equivalent circuit parameters with the constraints of positive values. The realized equivalent circuits of the windings can be determined. The validity of the combined algorithm is confirmed by comparison of the simulated results by the determined circuit model and the experimental results, and good agreement is observed. The proposed approach is very useful in lightning impulse tests on the reactor and transformer windings.

Keywords: lightning impulse voltage test; genetic algorithm; reactor and transformer windings; vector fitting

1. Introduction

Transformers and reactors are employed in a high-voltage (HV) system in many applications. The transformers are utilized for adjusting voltage levels in the AC transmission and distribution systems. The reactors are utilized for limitation of over voltage, reactive power compensation, tuned and detuned filters, and so on. During the operation of the transformers and the reactors, there are possibilities in insulation failure due to direct lightning and electromagnetic-induced lightning effects. Therefore, it is necessary to test the transformer and reactors with lightning impulse voltage for being an assessment of the insulation performance of the transformers and reactors before installation.

The crucial problem in the lightning impulse voltage tests on the transformer and reactor winding is the adjustment of the test voltage waveform according to the standard requirement. As shown in Figure 1, the front time (T_1), time to half (T_2), and overshoot rate (β_e) will be in the ranges of 1.2 µs ± 30% (0.84 µs to 1.56 µs), 50 µs ± 30% (40 µs to 60 µs), and less than 5%, respectively [1–5].
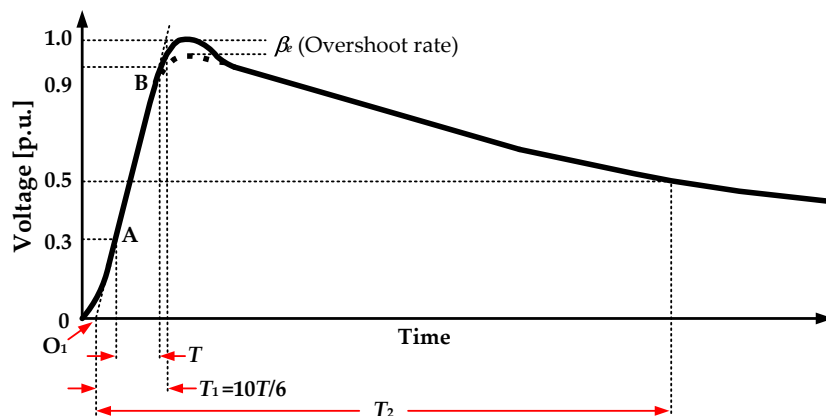
Figure 1. Generated lightning impulse voltage waveform.

Conventionally, the generator circuit named Marx's circuit, as shown in Figure 2, is applied in the lightning impulse voltage tests. The charging capacitance (C_s) will be much higher than load capacitance (C_b), since the efficiency of the circuit is necessary to be controlled at a high level (normally more than 90%). The spark gap (G) is used as a high-voltage switch. It will be sparked or switched on to connect the charging capacitor to the load for the generation of lightning impulse voltage. For the front time and time to half, according to the standard requirement, the front time and tail time resistances (R_d and R_e) can be calculated by Equations (1) and (2) [6].

$$R_d = \frac{T_1}{2.96}\left(\frac{C_s + C_b}{C_s C_b}\right) \tag{1}$$

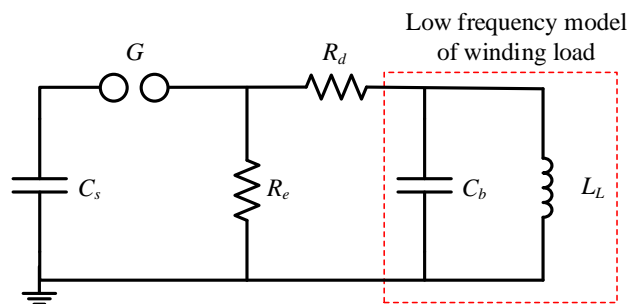$$R_e = \frac{T_1}{0.73}\left(\frac{1}{C_s + C_b}\right) \tag{2}$$

Figure 2. Conventional generator circuit used in the lightning impulse voltage tests, where C_s is a charging capacitor, G is a spark gap, R_e is a tail time resistor, R_d is a front time resistor, C_b is a load capacitor, and L_L is a load inductor.

Practically, in the low frequency range (below 10 kHz) the winding can be represented well by an equivalent circuit of an inductor in parallel with a capacitor. It is noticed by Glaninger that, if the inductance of the winding is less than 15 mH, the conventional circuit is quite difficult to apply and it is difficult to adjust T_2 to longer than 40 μs [7]. Therefore, Glaninger's generator circuit, as illustrated in Figure 3, is recommended to apply in the lightning impulse voltage test.

In Glaninger's circuit, as shown in Figure 3, the parallel connection of the additional inductor (L_d) with the front-time resistor (R_d) is used. This is for the purpose of extending the time to half in the impulse waveform. The parallel connection of the additional parallel resistor (R_p) with the test object is used for controlling the overshoot rate of the generated waveform. In 1978, K. Feser [8] proposed the approach for the selection of the appropriate circuit parameters—i.e. the charging capacitance (C_s),

the front-time resistance (R_d), the additional inductance (L_d), and the additional parallel resistance (R_p), as given in Equations (3) to (7). In addition, the appropriate tail-time resistor (R_e) has to be selected to obtain the undershoot voltage less than 50% of the peak voltage [7–11].

$$C_s \approx T_2^2/L_L \tag{3}$$

$$R_d = \left(0.4 \times 10^{-6}\right)/C_b \tag{4}$$

$$L_d = 1.25 \times 10^{-6} R_d \tag{5}$$

$$R_p = \left(R_d L_L\right)/L_d \tag{6}$$
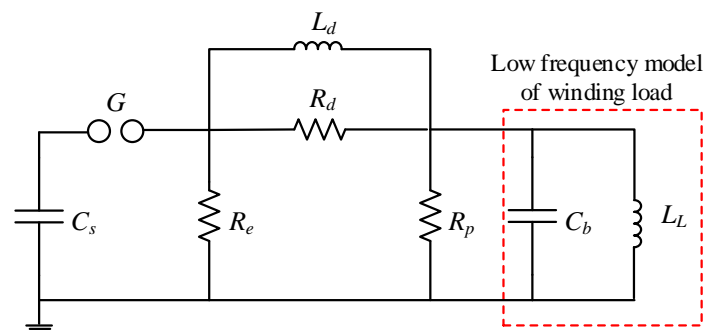
$$R_e = 1.6 \sqrt{L_L/C_s} \tag{7}$$

Figure 3. Glaninger's generator circuit for the lightning impulse voltage tests on the winding.

However, the distortion in the waveform generated by the circuit with parameters from K. Feser's suggestion was noted. A trial and error approach, then, is employed to adjust the circuit parameters to mitigate the waveform distortion and to obtain the waveform parameters, according to the standard requirement. An alternative method was proposed based on a neural network for the selection of appropriate Glaninger's circuit parameters [11].

Another concern is that impedance characteristics cannot be represented well by only simple lump elements throughout the frequency range of the applied lightning impulse voltage. Especially the frequency dependent impedance of the winding in the higher frequency range (>10 kHz) affects the waveform parameters—i.e. peak voltage, front time, time to half, and overshoot rate. In some cases, it is quite hard to adjust such waveform parameters according to the standard requirement [1–5]. In practice, for the generation of the standard lightning impulse voltages on the transformer and reactor windings, test engineers have to select appropriate components with their experience, and also make attempts with trial and error approaches. The damage on the windings and their insulation, therefore, can occur unintentionally during the process of the voltage waveform adjustment.

It is noted that the combination of an equivalent circuit of a transformer or reactor winding with circuit parameters of an impulse generator has to be taken into account so that the proper impulse voltage waveform can be generated during impulse tests. Simulation approaches have been proposed [12,13] to investigate the interaction between a transformer or reactor winding and the impulse generator circuits. These methods employ the results of frequency response analysis of the windings for computing multi-port networks and input impedances of the windings. The network impedances combined with the equivalent circuit of the impulse generator are utilized in the simulation in the frequency domain, and the results in the time domain can be obtained by inversed Laplace transformation. The generator circuit parameters are required to be adjusted to obtain the impulse voltage waveform according to the standard requirement. The results have shown that such methods provide very high accuracy. However, most of these methods require the construction of the complicated model and computation, and it also cannot be implemented directly to the circuit simulator. It is advantageous for

test engineers to use a circuit simulator, such as EMTP, to verify expected impulse voltage waveforms when performing impulse tests of the transformer or reactor windings. To implement cases on the circuit simulator, accurate equivalent circuits of the windings, as well as proper circuit components of the impulse generator, have to be identified. Therefore, the number of attempts for the waveform adjustment in the experiments will be reduced significantly, and the risk of the damage to the reactor under the waveform adjustment process is also reduced.

In this paper, an approach for a realized equivalent circuit identification of the transformer and reactor windings is presented. The determined equivalent circuit can be represented well by the characteristic in the lightning impulse voltage test. With the accurate circuit model, the effective approach based on the circuit simulation is also presented. The validity and accuracy of the proposed approach are ensured by comparison between simulated and experimental results. This paper is organized as follows. The identification of the accurate and realized equivalent circuit of the winding is presented in Section 2. The approach based on simulation for the lighting impulse voltage tests of the reactor and transformer windings is proposed in Section 3. Then, in Section 4, some study cases are considered, and the comparison of the results used the proposed method and experiments are presented for confirming the validity and accuracy of the proposed method. Finally, the conclusion is addressed in the final section.

2. Equivalent Circuit Identification

For the equivalent circuit identification, the impedance of a transformer or reactor winding was measured throughout the frequency range from 10 Hz to 10 MHz. The vector fitting [14] was employed to extract the equivalent circuit by matching the model impedance with the measured one. The equivalent circuit is composed of several series sets of RLC circuits, as shown in Figure 4.
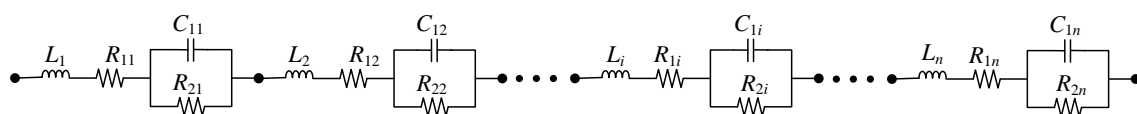

Figure 4. Equivalent circuit associated with complex conjugate pairs.

However, it is possible that negative circuit parameters can be found from the vector fitting. In this paper, the circuit components with the negative values were changed to be positive with the same absolute value. Such changed circuit components were set as starting values in a genetic algorithm with constraints of the only positive values. The genetic algorithm [15] was employed to search for the appropriate positive circuit parameters for obtaining the realized equivalent circuit and the guarantee of the passivity condition.

The brief details of the vector fitting and the genetic algorithm are presented as follows:

2.1. Vector Fitting

The vector fitting is an approach for fitting a rational function as expressed in Equation (8).

$$F(s) = es + d + \sum_{i=1}^{n} \left(\frac{res_i}{s - p_i} \right) \tag{8}$$

where, *F(s)* is the considered fitting rational function; *e* and *d* are real coefficients; res_i and p_i are the residue and the pole which can be either real numbers or complex conjugate pairs.

The approach has proven its performance in terms of stability, accuracy, and efficiency. The fine detail of the vector fitting approach can be found in [14].

For two rational terms with the complex conjugate pairs, the equivalent circuit can be represented, as illustrated in Figure 5, and the impedance with Laplace variable (s) of the equivalent circuit can be derived as Equation (9).

$$Z_i(s) = \frac{1}{C_{1i}} \frac{\left(s + \frac{R_1}{L_i}\right)}{\left(s^2 + \left(\frac{1}{R_{2i}C_{1i}} + \frac{R_1}{L_i}\right)s + \left(\frac{R_{1i}}{R_{2i}L_iC_{1i}} + \frac{1}{L_iC_{1i}}\right)\right)} \tag{9}$$
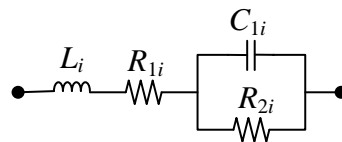

Figure 5. Equivalent circuit associated with complex conjugate pairs.

The circuit parameters associated with Figure 5 and Equation (9)—i.e., C_{1i}, R_{2i}, L_i, and R_{1i}—can be calculated from the poles (p_1 and p_2) and residues (res_1 and res_2) of the complex conjugate pairs using Equation (10) to (13), respectively.

$$C_{1i} = \frac{1}{(res_1 + res_2)} \tag{10}$$

$$R_{2i} = (res_1 + res_2) / \left[-(p_1 + p_2) + \frac{(res_1 p_2 + res_2 p_1)}{(res_1 + res_2)}\right] \tag{11}$$

$$L_i = \frac{(res_1 + res_2)}{p_1 p_2 + \left[-(p_1 + p_2) + \frac{(res_1 p_2 + res_2 p_1)}{(res_1 + res_2)}\right]} \times \frac{(res_1 + res_2)}{(res_1 p_2 + res_2 p_1)} \tag{12}$$

$$R_{1i} = \frac{L(res_1 p_2 + res_2 p_1)}{(res_1 + res_2)} \tag{13}$$

2.2. Genetic Algorithm

The genetic algorithm is a random-based classical evolutionary algorithm, which is often used for solving the constrained and unconstrained optimization problems. A simple genetic algorithm [15,16] applied in this paper relies on the process of natural selection, which is composed of reproduction, selection, crossover, and mutation. In this paper, parameter estimation based on a genetic algorithm (GA) [15,16] is employed to search for the most appropriate circuit parameters, in which the impedances of the transformer or reactor winding from calculation using the equivalent circuit model and experiment are matched. The objective function ($Ob(X)$), which the genetic algorithm uses in the minimization, is shown in Equation (14).

$$Ob(X) = \sum_{k=1}^{n} \left(Z_{o(\exp)}(k) - Z_{o(\text{sim})}(X,k)\right)^2 \tag{14}$$

where, X is the unknown circuit parameters—i.e. C_{1i}, R_{2i}, L_i, and R_{1i}; $Z_{o(\exp)}$ and $Z_{o(\text{sim})}$ are the impedances from the experiment and the simulation model using the lumped circuit model, as shown in Figure 4; k is the k th frequency point, and n is the number of frequency points of the measured and simulated impedances. Only positive values of the parameters were set as the constraints in the genetic algorithm. The flowchart of parameter optimization for searching the proper circuit parameters by the genetic algorithm is shown in Figure 6.
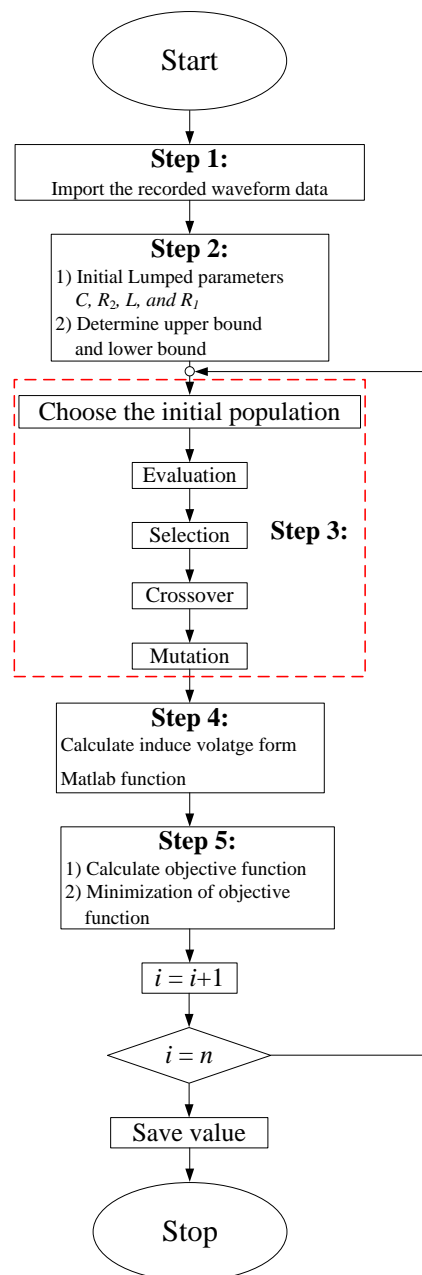
Figure 6. Flowchart of the proposed algorithm.

3. Procedures of the Effective Approach

The procedure of the proposed method starts from the measurement of the input impedance of the considered winding. The impedance analyzer, shown in Figure 7, is used to measure the input impedance from the frequency range of 10 Hz to 10 MHz. Figure 7 also shows the example of the experimental set up for the measurement of input impedance of the reactor and transformer windings.
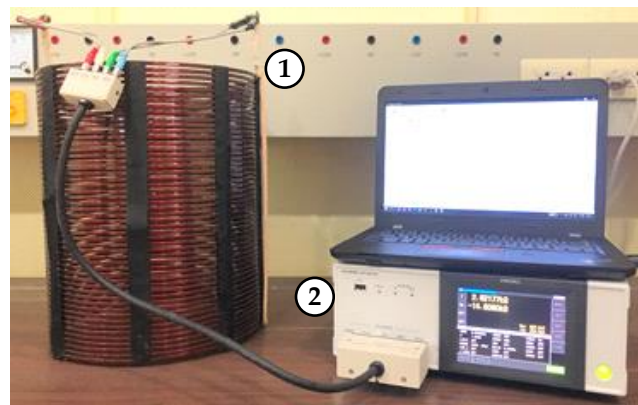
(a)
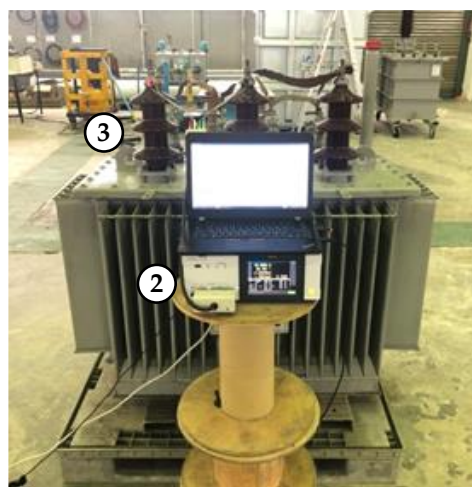
(b)

Figure 7. Experimental set up for measuring input impedance of the windings, where (1) is the winding under test, (2) is the impedance analyzer, and (3) is the transformer under test. (**a**) Reactor winding under tests. (**b**) Transformer winding under tests.

The flowchart of the proposed approach is presented in Figure 8. In steps 1 and 2, the proposed approach is initiated from the identification of the realized equivalent circuit of the considered winding, as presented in Section 2. Then, the generator circuit is selected from the criteria of the low frequency inductance (L_L), which can be determined from the impedance in the low frequency range from 1 kHz to 5 kHz. When L_L is less than 15 mH, the Glaninger circuit, as shown in Figure 3, will be recommended to represent the generator circuit [7]. For other values of L_L, the conventional circuit in Figure 2 will be selected as the generator circuit. From the identified equivalent circuit of the winding and the selected generator circuit parameters, the circuit simulator is utilized to compute the generated waveform, and the waveform parameters are evaluated according to the standards, IEC 60060-1 [1] and IEC 61083 [17–20]. If the waveform parameters are not in accordance with the standard requirement, the circuit parameters of the generator circuit will be adjusted until the waveform parameters are required by the standard are obtained. The determined generator circuit parameters are employed in the actual lightning impulse voltage tests.
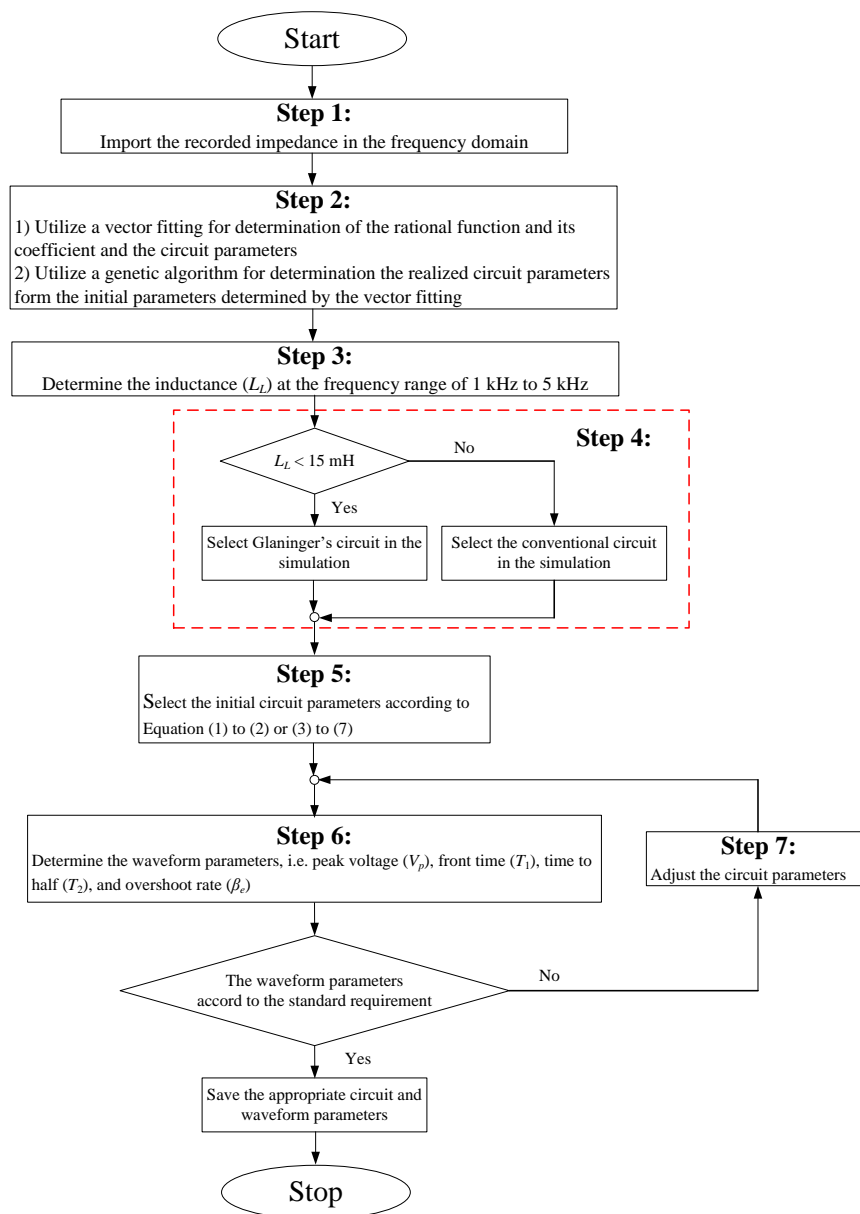
Figure 8. Flowchart of the proposed approach for determination of the generator circuit parameters.

4. Case Studies

To validate and investigate the accuracy of the proposed approach, case studies were performed on a reactor, a power transformer, and two distribution transformers.

4.1. Reactor

In this case, a reactor with an inductance of 1.3 mH was considered. With the proposed approach, the equivalent circuit of an air-core reactor was extracted from the measured input impedance of the reactor. The number of RLC sets was four, as shown in Figure 9. The circuit parameters determined by the vector fitting and proposed algorithms are expressed in Tables 1 and 2. It is found that some parameters determined by the vector fitting algorithm are negative real, and the proposed algorithm (combination of the vector fitting and genetic algorithms) can find the realized appropriate circuit parameters (positive real). The good agreement between impedances from the experiment and the equivalent circuit model are observed and shown in Figures 10 and 11.
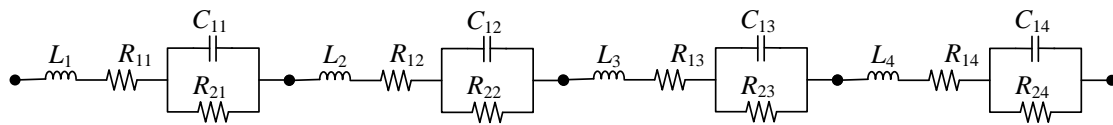
Figure 9. An extracted equivalent circuit of an air-core reactor.

Table 1. Circuit parameters determined by the vector fitting approach.

Section No.	Circuit Parameters			
	R_{1i} (Ω)	L_i (mH)	R_{2i} (kΩ)	C_i (pF)
1	42.95	0.0239	40.18	85.57
2	−13.86	0.0860	13.80	659.30
3	−15.05	0.1087	6.649	532.60
4	−22.43	1.1680	30.24	663.90

Table 2. Circuit parameters determined by the proposed approach.

Section No.	Circuit Parameters			
	R_{1i} (Ω)	L_i (mH)	R_{2i} (kΩ)	C_i (pF)
1	0.000	0.0079	0.309	268.20
2	0.001	0.0224	4.286	549.40
3	0.001	0.1087	13.030	532.60
4	0.021	1.1680	49.190	663.90
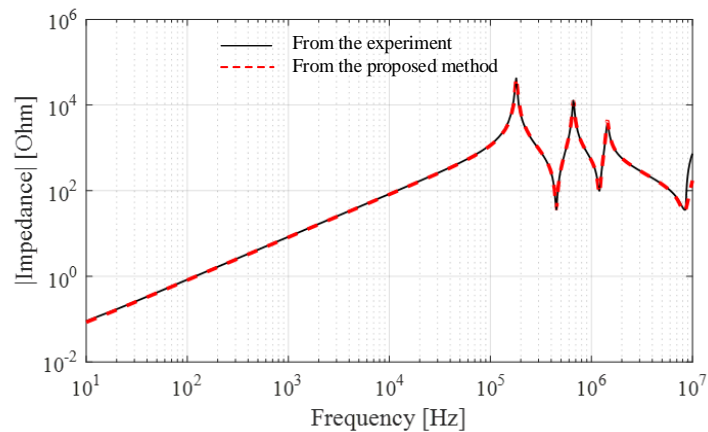
Figure 10. Magnitude of input impedances of the reactor from the measurement and the proposed method.
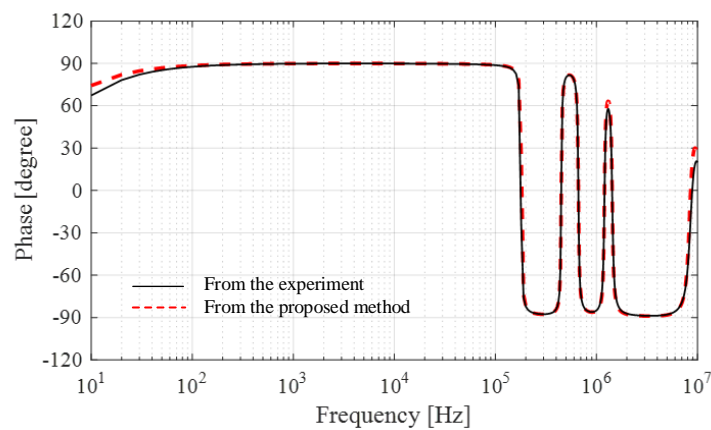

Figure 11. Phase of input impedances of the reactor from the measurement and by the proposed method.

This determined model has to be employed in combination with an impulse voltage generation circuit. From the flowchart shown in Figure 8, in the case that the inductance is less than 15 mH, Glaninger's circuit must be employed for impulse voltage generation [7]. To present the necessity of Glaninger's circuit for the generation of the standard lighting impulse voltage waveform on the low inductance load, the determined model with the conventional generator circuit is considered. In this case the capacitance of the model is quite low (less than 1 nF), so it is necessary to add a load capacitance (C_b) of 2 nF in the generation circuit. In case 1, the charging capacitance was set to be 0.5 μF, and the calculated front and tail time resistances (R_d and R_e) by Equations (1) and (2) are 200 Ω and 150 Ω, respectively. As shown in Figure 12, the front time and time to half are 1.23 μs and 5.57 μs, respectively. Based on the conventional circuit, to increase the time to half the R_e and C_s should be increased. In case 2, R_e was set to be infinity or no tail time resistor connected in the generator circuit. The front time and time to half are 1.29 μs and 6.30 μs, respectively. In case 3, there was no tail time resistor connected in the generator circuit and C_s was changed to be 3 μF, but the front time and time to half are 1.30 μs and 6.62 μs, respectively. All generated waveforms are presented in Figure 12. It can be concluded that the conventional circuit is not appropriate to use in the generation of the standard lightning impulse voltage in the cases of low inductance loads.
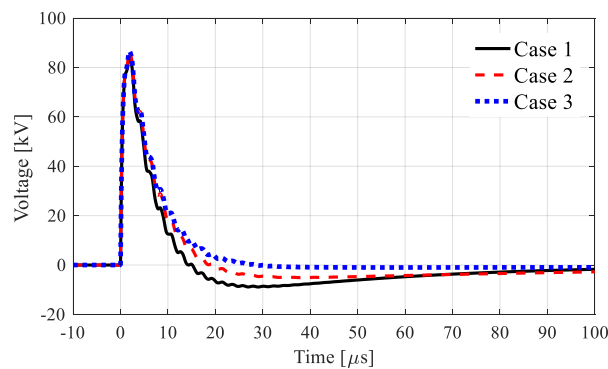

Figure 12. Generated waveforms by the conventional circuit.

The equivalent circuit of the completed test system (an identified model and an impulse generator circuit) is presented in Figure 13. Additionally, the experimental set up for lightning impulse voltage generation on the reactor is shown in Figure 14. The initial impulse generator circuit parameters are calculated by Equation (3) to (7). The generated waveform with these circuit parameters is not in accordance with the standard requirement, so these parameters required further adjustment. The proper circuit parameters are given in Table 3. Good agreement of the simulated and experimental voltage waveforms is observed, and the results are shown in Figure 15. The front time (T_1), the time to half (T_2), and the overshoot rate (β_e) collected from the experiment are 1.35 μs, 42.0 μs, and 4.60%, respectively, whereas T_1, T_2, and β_e from the simulation using the proposed model are 1.51 μs, 42.3 μs, and 3.11%, respectively. These parameters are in the accepted ranges of the standard requirement.
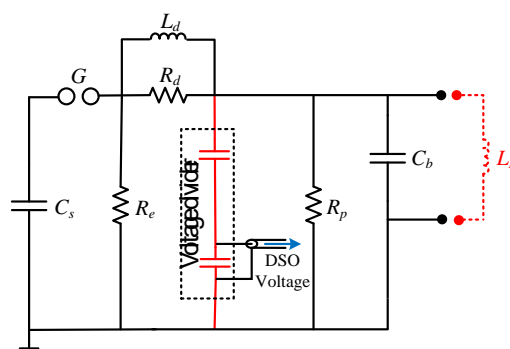

Figure 13. Equivalent circuit of the completed test system for the lightning impulse test of the reactor.
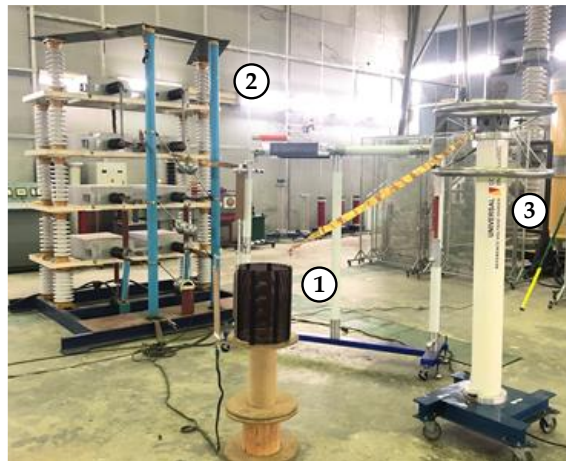
Figure 14. Experimental set up of the completed test system for the lightning impulse test of the reactor, where (1) is the reactor under test, (2) is the impulse voltage generator, and (3) is a voltage divider.

Table 3. Selected circuit parameters of the lightning impulse voltage generation circuit.

Circuit Parameters					
C_s (µF)	R_e (Ω)	L_d (µH)	R_d (Ω)	R_p (Ω)	C_b (nF)
3.0	40.0	100.0	200.0	250.0	2.0
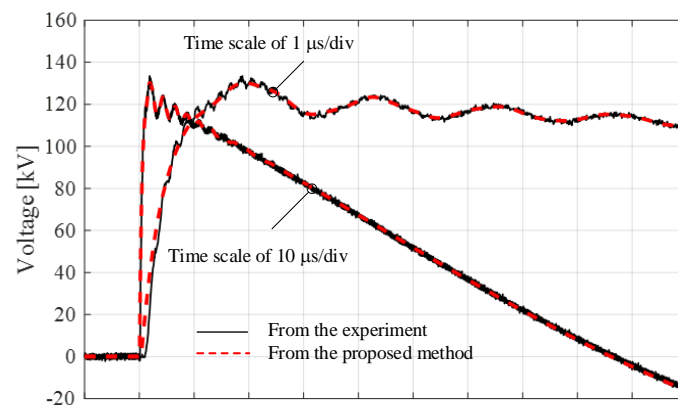
Figure 15. Comparison of the generated impulse voltage waveforms collected from the experiment and computed by the proposed method.

4.2. Power Transformer

In this case, a power transformer (60 MVA 115 kV/24 kV) was considered. With the proposed approach, the equivalent circuit of a 24-kV winding was extracted. The number of RLC sets was four, as shown in Figure 9. The realized circuit parameters are expressed in Table 4. The good agreement between impedances from the experiment and the equivalent circuit model are observed and shown in Figures 16 and 17.

Table 4. Circuit parameters determined by the proposed approach.

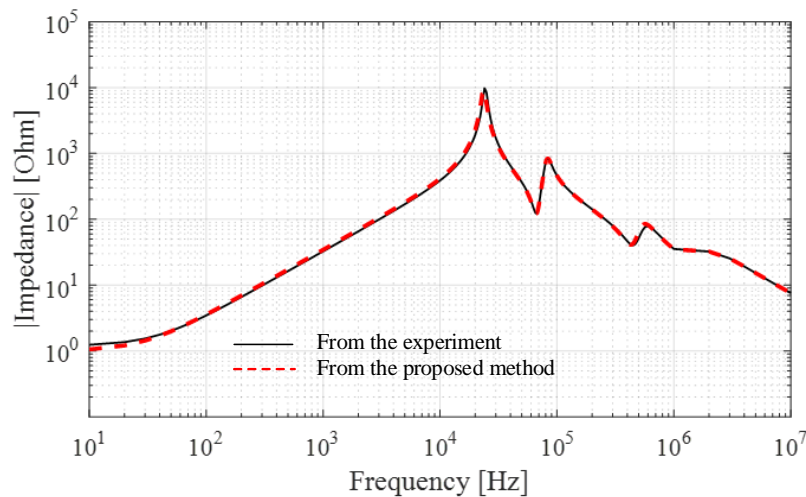| Section No.	Circuit Parameters			
	R_{1i} (Ω)	L_i (mH)	R_{2i} (kΩ)	C_i (nF)
1	0.000	0.0018	0.021	4.450
2	0.101	0.0063	0.061	14.130
3	0.402	0.2350	0.819	16.120
4	0.515	5.2400	10.120	8.663

Figure 16. Magnitude of input impedances of the transformer winding from the measurement and the proposed method.
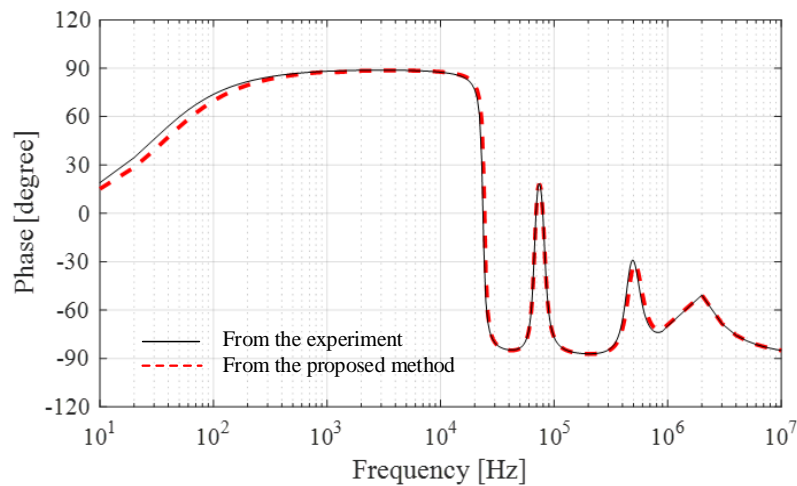

Figure 17. Phase of input impedances of the transformer winding from the measurement and by the proposed method.

This determined model was employed in the proposed method in lightning impulse voltage test. As with the procedure in Section 3, the low frequency inductance of 5.58 mH was computed. Therefore, Glaninger's circuit is recommended to employ as an impulse voltage generation circuit. The equivalent circuit of the completed test system (an identified model and an impulse generation circuit) is presented in Figure 18. The initial impulse generator circuit parameters are calculated by Equations (3) to (7). The generated waveform with these circuit parameters is not in accordance with the standard requirement, so these parameters require further adjustment. The proper circuit parameters are given in Table 5. The good agreement of the simulated and experimental voltage waveforms is observed, and the results are shown in Figure 19. The front time (T_1), the time to half (T_2), and the overshoot rate (β_e) collected from the experiment are 1.15 µs, 41.0 µs, and 4.23%, respectively, whereas T_1, T_2, and β_e from the simulation using the proposed model are 1.41 µs and 41.9 µs, and 3.32%, respectively. These parameters are in the accepted ranges of the standard requirement.
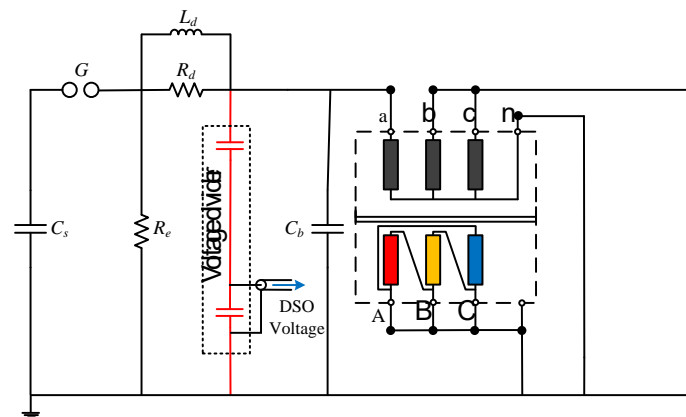
Figure 18. Equivalent circuit of the completed test system for the lightning impulse test of the power transformer winding.

Table 5. Selected circuit parameters of the lightning impulse voltage generation circuit.

Circuit Parameters					
C_s (µF)	R_e (Ω)	L_d (µH)	R_d (Ω)	R_p (Ω)	C_b (nF)
1.0	600.0	100.0	40.0	100.0	0.0
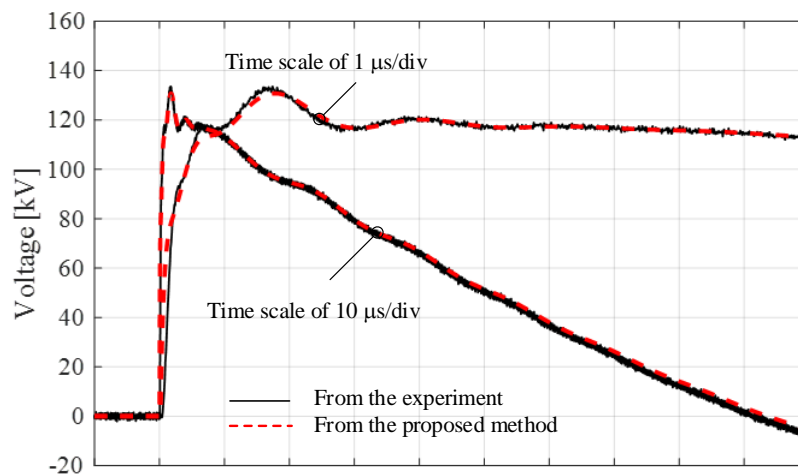
Figure 19. Comparison of the generated impulse voltage waveforms collected from the experiment and computed by the proposed method.

4.3. Distribution Transformer

In this part, two distribution transformers are considered. In the first case of the distribution transformers, a distribution (2 MVA 420 V/24 kV) was considered. With the proposed approach, the equivalent circuit of a 24-kV winding was extracted. The number of RLC sets was 3. The realized circuit parameters are expressed in Table 6. The good agreements between impedances from the experiment and the equivalent circuit model are observed and shown in Figures 20 and 21.

Table 6. Circuit parameters determined by the proposed approach.

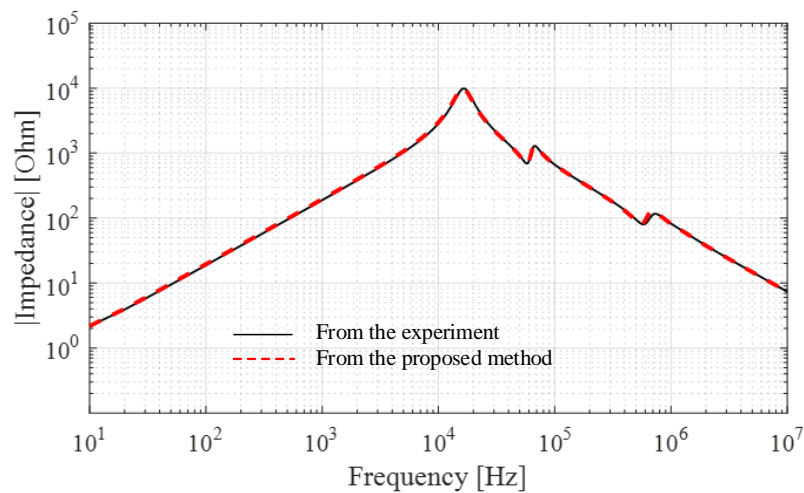| Section No.	Circuit Parameters			
	R_{1i} (Ω)	L_i (mH)	R_{2i} (kΩ)	C_i (nF)
1	0.00	0.0054	0.071	11.30
2	0.06	0.3352	0.767	18.10
3	0.95	31.0200	9.876	3.13

Figure 20. Magnitude of input impedances of the transformer winding from the measurement and the proposed method.
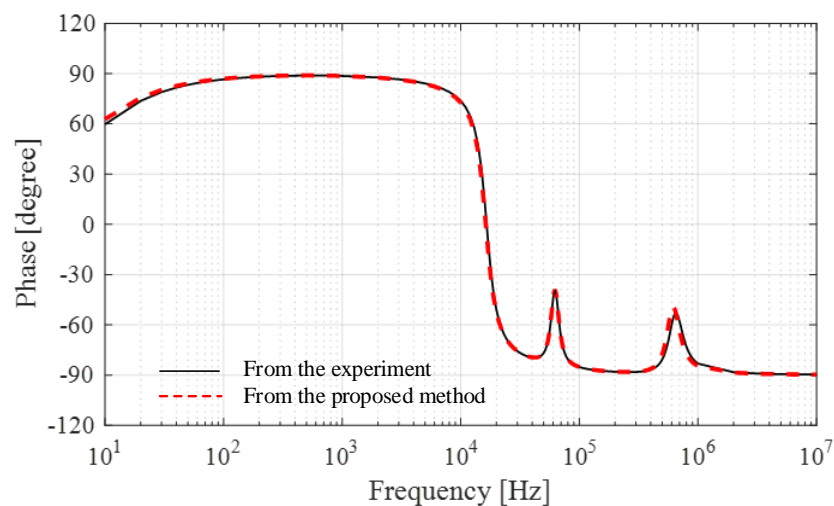

Figure 21. Phase of input impedances of the transformer winding from the measurement and by the proposed method.

This determined model was employed in the proposed method in lightning impulse voltage test. As with the procedure in Section 3, the low frequency inductance of 31.0 mH was computed. Therefore, the conventional circuit, as shown in Figure 2, is recommended as an impulse voltage generation circuit. The equivalent circuit of the completed test system (an identified model and an impulse generation circuit) is presented in Figure 22, and the experimental set up is also presented in Figure 23. The initial generator circuit parameters are calculated by Equations (1) to (2). The generated waveform with these circuit parameters is not in accordance with the standard requirement, so these parameters are required for further adjustment. The proper circuit parameters are given in Table 7. Good agreement of the simulated and experimental voltage waveforms is observed, and the results are shown in Figure 24. The front time (T_1), the time to half (T_2), and the overshoot rate (β_e) collected from the experiment are 1.02 μs, 52.5 μs, and 3.52%, respectively, whereas T_1, T_2, and β_e from the simulation using the proposed model are 1.21 μs and 53.9 μs, and 1.71%, respectively. These parameters are in the accepted ranges of the standard requirement.
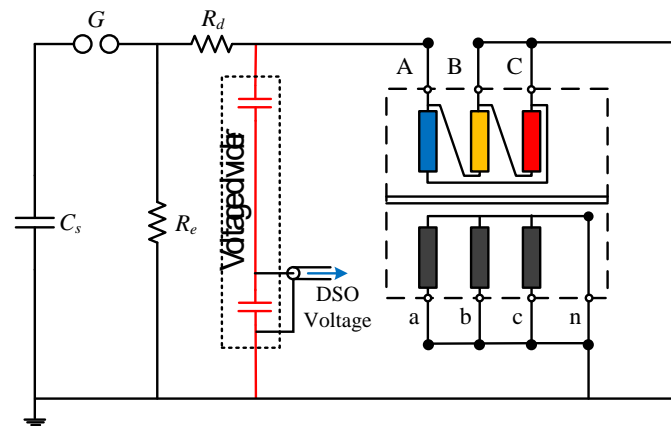
Figure 22. Equivalent circuit of the completed test system for the lightning impulse test of the distribution transformer winding.
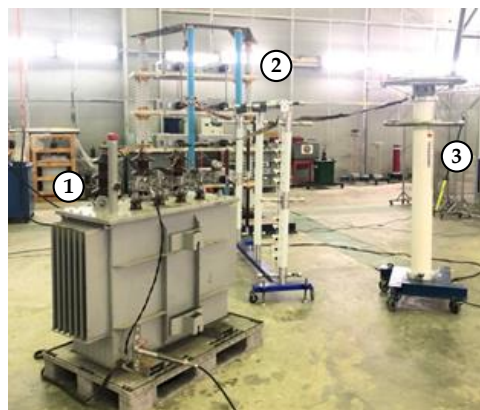

Figure 23. Experimental set up of the completed test system for the lightning impulse test of the distribution transformer winding, where (1) is the transformer under test, (2) is the impulse voltage generator, and (3) is a voltage divider.

Table 7. Selected circuit parameters of the lightning impulse voltage generation circuit.

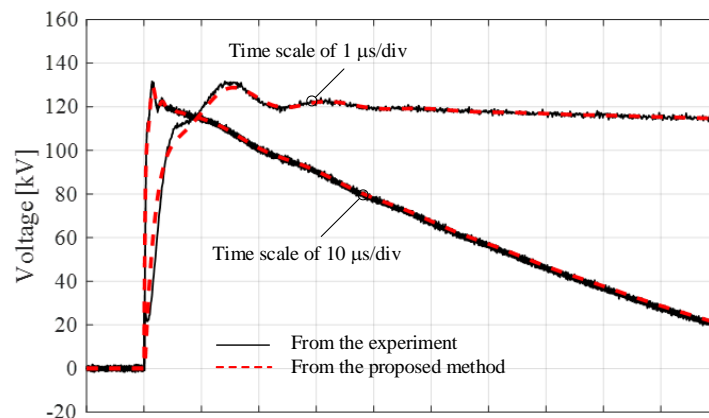| Circuit Parameters			
C_s (μF)	R_e (Ω)	R_d (Ω)	C_b (nF)
0.5	300.0	100.0	0.0

Figure 24. Comparison of the generated impulse voltage waveforms collected from the experiment and computed by the proposed method.

In the second case of the distribution transformers, a distribution (250 kVA 420V/22 kV) was considered. With the proposed approach, the equivalent circuit of a 22-kV winding was extracted. The number of RLC sets was 2. The realized circuit parameters are expressed in Table 8. The good agreements between impedances from the experiment and the equivalent circuit model are observed and shown in Figures 25 and 26.

Table 8. Circuit parameters determined by the proposed approach.

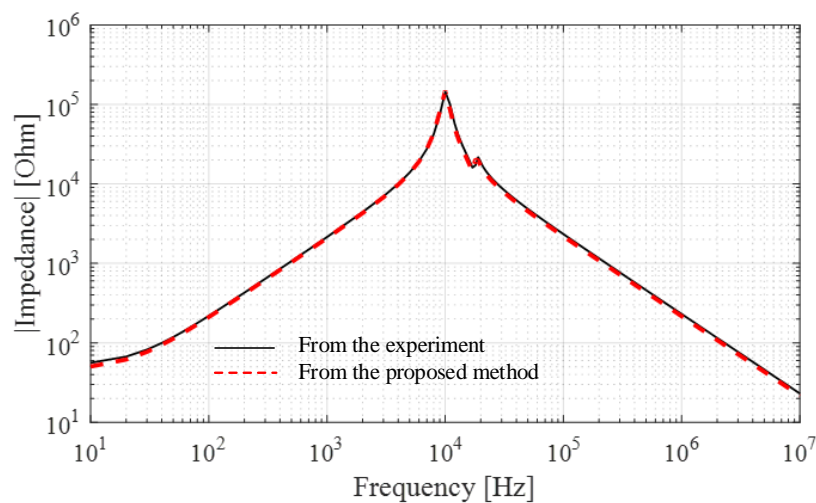| Section No.	Circuit Parameters			
	R_{1i} (Ω)	L_i (mH)	R_{2i} (kΩ)	C_i (nF)
1	2.42	7.353	9.752	10.02
2	48.3	331.2	159.09	0.741

Figure 25. Magnitude of input impedances of the transformer winding from the measurement and the proposed method.
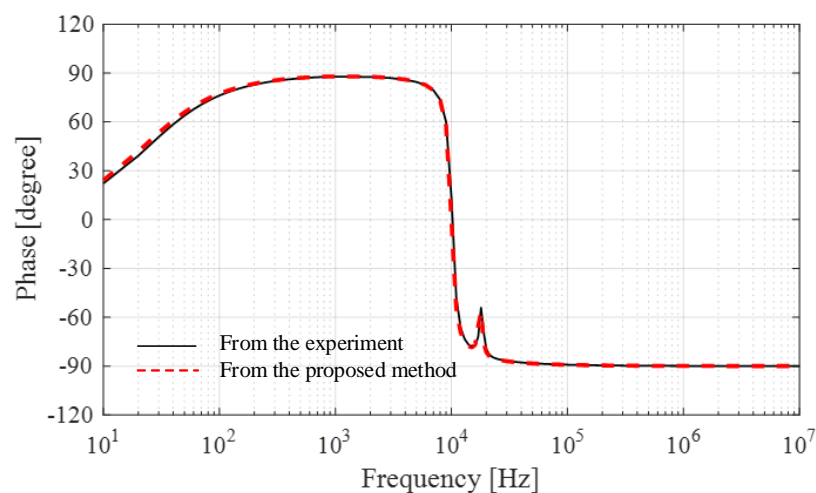

Figure 26. Phase of input impedances of the transformer winding from the measurement and by the proposed method.

This determined model was employed in the proposed method in a lightning impulse voltage test. As with the procedure in Section 3, the low frequency inductance of 320.3 mH was computed. Therefore, the conventional circuit, as shown in Figure 2, is recommended as an impulse voltage generation circuit. The equivalent circuit of the completed test system (an identified model and an impulse generation circuit) is presented in Figure 22. The initial generator circuit parameters,

calculated by Equations (1) to (2), can be used for lightning impulse voltage properly. The proper circuit parameters are given in Table 9. Good agreement of the simulated and experimental voltage waveforms is observed, and the results are shown in Figure 27. The front time (T_1), the time to half (T_2), and the overshoot rate (β_e) collected from the experiment are 1.15 µs, 45.1 µs, and 0.52%, respectively, whereas T_1, T_2, and β_e from the simulation using the proposed model are 1.09 µs and 43.9 µs, and 0.61%, respectively. These parameters are in the accepted ranges of the standard requirement.

Table 9. Selected circuit parameters of the lightning impulse voltage generation circuit.

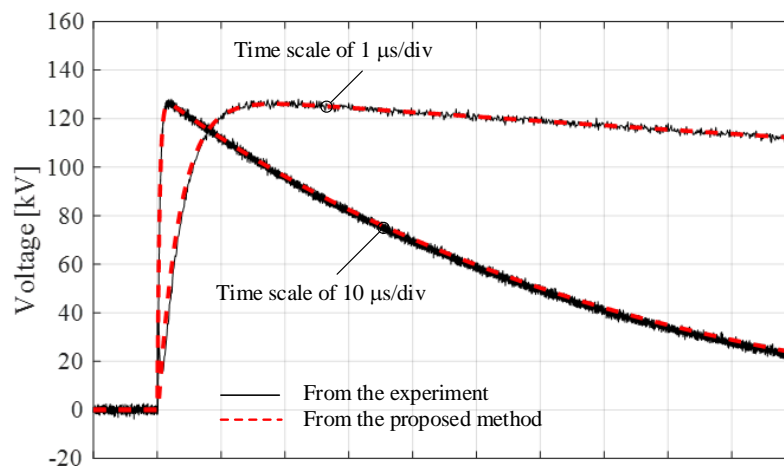| Circuit Parameters			
C_s (µF)	R_e (Ω)	R_d (Ω)	C_b (nF)
0.5	150.0	500.0	0.0

Figure 27. Comparison of the generated impulse voltage waveforms collected from the experiment and computed by the proposed method.

5. Conclusions

In this paper, the effective simulation approach for lightning impulse voltage tests of transformer and reactor windings has been proposed. In this approach, a combination between an accurate wide frequency model (10 Hz to 10 MHz) of transformer as well as reactor windings and the proper impulse generation circuit has been described. For the realized equivalent identification of the windings, the combined methods of the vector fitting and the genetic algorithm have been employed. The vector fitting has been utilized to determine the starting circuit parameters, and the genetic algorithm has been employed to search for the realized circuit parameters (positive values). Case studies have been performed on a reactor, a power transformer, and two distribution transformers. Additionally, experiments have been carried out to confirm the validity of the proposed approach. From the good agreements of the simulated and the experimental results, the validity with a promising accuracy has been confirmed. It has been shown that the realized circuit parameters of the winding high frequency model function very well with the proper impulse generation circuits (both Glaninger's circuit and conventional circuit) in effective simulation approaches for impulse voltage testing on transformers and reactors. From this achievement, the possibility of the damage on the windings and their insulation occurring unintentionally during the process of the voltage waveform adjustment will be reduced significantly.

References

1. IEC 60060-1. *High-Voltage Test Techniques. Part 1: General Definitions and Test Requirements*, 3rd ed.; International Electrotechnical Commission (IEC): Geneva, Switzerland, 2010.

2. IEEE Standard 4TM-2013. *IEEE Standard for High-Voltage Testing Techniques*; Institute of Electrical and Electronics Engineers (IEEE): Piscataway, NJ, USA, 2013.

3. IEC 60076-1. *Power Transformer. Part 1: General*, 3rd ed.; International Electrotechnical Commission (IEC): Geneva, Switchzerland, 2011.

4. IEC 60076-3. *Power Transformer. Part 3: Insulation Level, Dielectric Tests and External Clearances in Air*, 3rd ed.; International Electrotechnical Commission (IEC): Geneva, Switchzerland, 2013.

5. IEC 60076-4. *Power Transformer. Part 4: Guide to the Lightning Impulse and Switching Impulse Testing—Power Transformer and Reactors*, 1st ed.; International Electrotechnical Commission (IEC): Geneva, Switchzerland, 2002.

6. Kuffel, E.; Zaengl, W.S.; Kuffel, J. *High Voltage Engineering: Fundamentals*, 2nd ed.; Newnes: Oxford, UK, 2000.

7. Glaninger, P. Impulse testing of low inductance electrical equipment. In Proceedings of the 2nd International Symposium on High Voltage Technology, Zurich, Switzerland, 9–13 September 1975; pp. 140–144.

8. Feser, K. Circuit Design of Impulse Generators for the Lightning Impulse Voltage Testing of Transformers. Bulleytin SEV/VSE Bd 1987. Available online: www.haefely.com (accessed on 15 November 2019).

9. Schrader, W.; Schufft, W. *Impulse Voltage Test of Power Transformers*; paper No. 13; HV Technologies, Inc.: Manassas, VA, USA, 2000.

10. Karthikeyan, B.; Rajesh, R.; Balasubramanian, M.; Saravanan, S. Experimental investigations on IEC suggested methods for improving waveshape during impulse voltage testing. In Proceedings of the 2006 IEEE 8th International Conference on Properties & applications of Dielectric Materials, Bali, Indonesia, 26–30 June 2006.

11. Tuethong, P.; Kitwattana, K.; Yutthagowith, P.; Kunakorn, A. An algorithm for circuit parameter Identification in lightning Impulse voltage generation for low-inductance loads. *Energies* **2020**, *13*, 3913. [CrossRef]

12. Mirzaei, H. A Simple Fast and Accurate Simulation Method for Power Transformer Lightning Impulse Test. *IEEE Trans. Power Deliv.* **2019**, *33*, 1151–1160. [CrossRef]

13. Mirzaei, H.; Bayat, F.; Miralikhani, K. A Semi-Analytic Approach for Determining Marx Generator Optimum Set-up during Power Transformers Factory Test. *IEEE Trans. Power Deliv.* **2020**. Early Access. [CrossRef]

14. Gustavsen, B.; Semlyen, A. Rational approximation of frequency domain responses by vector fitting. *IEEE Trans. Power Deliv.* **1999**, *14*, 1052–1061. [CrossRef]

15. Yang, X. *Engineering Optimization: An Introduction with Metahueristic Applications*; John Wiley & Sons, Inc.: Hoboken, NJ, USA, 2010; pp. 173–176.

16. Mehdi, B.; Davood, A.; Hassan, B.; Ebrahim, R. Identification of Transient Model Parameters of Transformer Using Genetic Algorithm. In Proceedings of the International Conference on Power System Technology, Hangzhou, China, 24–28 October 2010; pp. 1–6.

17. IEC 61083-2. *Instruments and Software used for Measurement in High-Voltage and High Current Tests. Part 2: Requirements for Software for Tests with Impulse Voltages and Currents*, 2nd ed.; International Electrotechnical Commission (IEC): Geneva, Switchzerland, 2013.

18. Pattanadech, N.; Yutthagowith, P. Fast curve fitting algorithm for parameter evaluation in lightning impulse test technique. *IEEE Trans. Dielectr. Electr. Insul.* **2015**, *22*, 2931–2936. [CrossRef]

19. Yutthagowith, P.; Pattanadech, N. Improved least-square prony analysis technique for parameter evaluation of lightning impulse voltage and current. *IEEE Trans. Power Deliv.* **2016**, *31*, 271–277. [CrossRef]

20. Yutthagowith, P.; Tuethong, P.; Pattanadech, N. Effective circuit parameter determination in lightning impulse voltage tests of air core inductors. In Proceedings of the 12th IET International Conference on AC and DC Power Transmission, Beijing, China, 28–29 May 2016.

Publisher's Note: MDPI stays neutral with regard to jurisdictional claims in published maps and institutional affiliations.